

# Partially Hidden Markov Models for Privacy-preserving Modeling of Indoor Trajectories

Aditya Jitta<sup>a</sup>, Arto Klami<sup>a</sup>

<sup>a</sup>*Helsinki Institute for Information Technology HIIT,  
Department of Computer Science, University of Helsinki*

---

## Abstract

Markov models are natural tools for modeling trajectories, following the principle that recent location history is predictive of near-future directions. In this work we study Markov models for describing and predicting human movement in indoor spaces, with the goal of modeling the movement on a coarse scale to protect the privacy of the individuals. Modern positioning devices, however, provide location information on a much more finer scale. To utilize this additional information we develop a novel family of partially hidden Markov models that couple each observed state with an auxiliary side information vector characterizing the movement within the coarse grid cell. We implement the model as a nonparametric Bayesian model and demonstrate it on real-world trajectory data collected in a hypermarket.

*Keywords:* Hierarchical Dirichlet process, Markov models, Movement trajectories, Nonparametric Bayesian inference, Privacy

---

## 1. Introduction

Human movement in indoor spaces can be reliably tracked with various localization techniques, such as wireless network signal strength [1, 2], dead reckoning [3], or locally deployed high-accuracy positioning systems often based on Bluetooth smart [4]. The state-of-the-art solutions can localize individuals with sufficient accuracy to know where exactly they are in some complex indoor space, such as a museum, hypermarket, or other public place. The measurement

8 error of the most accurate systems is measured in the range of 0.1-1 meters, and  
9 is hence comparable or smaller than the personal space of an individual. For  
10 many practical purposes the localization can therefore be considered error-free.

11 Given access to location data, a natural question to consider is modeling of  
12 movement trajectories, either to describe movement patterns within the building  
13 or to attempt predicting future locations based on already observed locations of  
14 an individual. In recent years models for indoor trajectories have been presented  
15 based on various alternative modeling approaches: For example, Nielsen et al. [5]  
16 used hidden Markov models for movement trajectories to improve localization  
17 accuracy, Yoo et al. [6] used Gaussian process models for trajectories to learn  
18 a map of the building, and Nianyin et al. [7] used particle swarm optimization  
19 for planning robot trajectories.

20 Our work falls into the same general category: We model indoor movement  
21 trajectories based on high-accuracy positioning data, building models for both  
22 descriptive and predictive analysis. Our goal is to design justified and auto-  
23 mated Bayesian tools for this task, without requiring or revealing too detailed  
24 information about the individuals. Even though the measurement devices can  
25 provide near-perfect positioning accuracy, the typical use cases for the premise  
26 owners, such as targeted advertising or collecting statistics on movement pat-  
27 terns, do not require knowing the exact positions. In most cases it is enough  
28 to know that the client is, for example, browsing the dairy section of a mar-  
29 ket, whereas the knowledge that they are currently handling a specific product  
30 might be considered intrusive. To preserve the privacy of the customers, it hence  
31 makes sense to consider models that do not reveal or even require storing the  
32 exact locations.

33 The easiest privacy-preserving solution is to discretize the locations on a  
34 sufficiently coarse scale, effectively mimicking the kind of data a less accurate  
35 positioning tool would provide. This is naturally not optimal since it completely  
36 ignores the improved positioning accuracy. In this work we build models that  
37 are fundamentally based on discretization, but that complement the discretized  
38 coarse locations (called cells) with aggregate summary statistics based on the

39 high-accuracy positioning data. These summaries intend to capture the nature  
40 of the movement within the cell, without retaining the actual detailed coordi-  
41 nates. For learning the model we then only need to store the information on  
42 which cell the person is in, coupled with these summary statistics, without pro-  
43 viding further access to the raw high-accuracy coordinates. Ideally the summary  
44 statistics would be computed already at the level of the positioning system itself  
45 so that the raw coordinates could be discarded in real time, to best guarantee  
46 that the privacy of the users is not compromised.

47 Markov Models (MM) that assume the next state depends solely on the  
48 current state are computationally tractable tools for modeling trajectories over  
49 such discrete observed states, and have been used as a crude approximation for  
50 human mobility trajectories as well [8]. For improved accuracy, we should typi-  
51 cally model also higher-order transitions, conditioning the expected movements  
52 not only on the latest state but on a sequence of the recent states, for example  
53 using variable-order MMs [9, 10]. While Markov models are indeed good tools  
54 for predicting future movements, they completely ignore the detailed movement  
55 within the cells.

56 In this work we extend MMs to support also the auxiliary statistics, via a  
57 latent state formulation. We provide for each cell a collection of latent states  
58 that generate the auxiliary statistics, and further condition the transition prob-  
59 abilities to the next cell not only on the observed state history but also on the  
60 latent state. Even though the abstract formulation reminds the concept of hid-  
61 den Markov models (HMM) [11] and our inference borrows some key elements  
62 from HMM literature, it differs fundamentally in two respects: The latent states  
63 are conditional on the observed states (and not vice versa as in HMMs), and  
64 the model efficiently supports higher-order transitions.

65 We call the model partially hidden Markov model (PHMM), since the dy-  
66 namics operate on the combination of the observed discrete states and the latent  
67 states conditional on those. We implement the model within the nonparamet-  
68 ric Bayesian framework, using a three-level extension of hierarchical Dirichlet  
69 process (HDP) [12, 13] for determining the local state cardinalities and beam

70 sampling [14] for the latent state inference. We evaluate the model on artificial  
71 data, and then proceed to demonstrate its use in modeling actual high-precision  
72 indoor data collected in a hypermarket during a period of one month. We illus-  
73 trate how the model naturally provides interpretable summaries of movement  
74 patterns within the space via the latent states, and that it can predict future  
75 movements of the individuals.

76 The main contributions of this work can be summarized as:

- 77 • Introduction of the novel PHMM model that extends Markov models by  
78 complementing them with latent states that influence both the transition  
79 probabilities and emission probabilities for feature vectors associated with  
80 the observed discrete states, improving both interpretability and predic-  
81 tion accuracy.
- 82 • Non-parametric Bayesian implementation of PHMM to automatically deter-  
83 mine the required number of latent states, and generalization of the  
84 PHMM model for higher-order histories.
- 85 • Use of PHMM for modeling indoor movement trajectories in a privacy-  
86 preserving manner; instead of modeling raw coordinates we model move-  
87 ment along coarse grid that does not reveal unnecessarily detailed infor-  
88 mation about the user, while using the detailed coordinates only to create  
89 a feature vector characterizing the type of movement within each grid cell.

## 90 **2. Background**

91 Before describing the proposed model, we briefly cover the necessary back-  
92 ground. We introduce first the most closely related models to enable under-  
93 standing how the partially hidden Markov model is related to regular and hid-  
94 den Markov models, as well as dynamic Bayesian networks in general, and then  
95 give a quick overview to the mathematical tools used when building the non-  
96 parametric PHMM in Section 3.

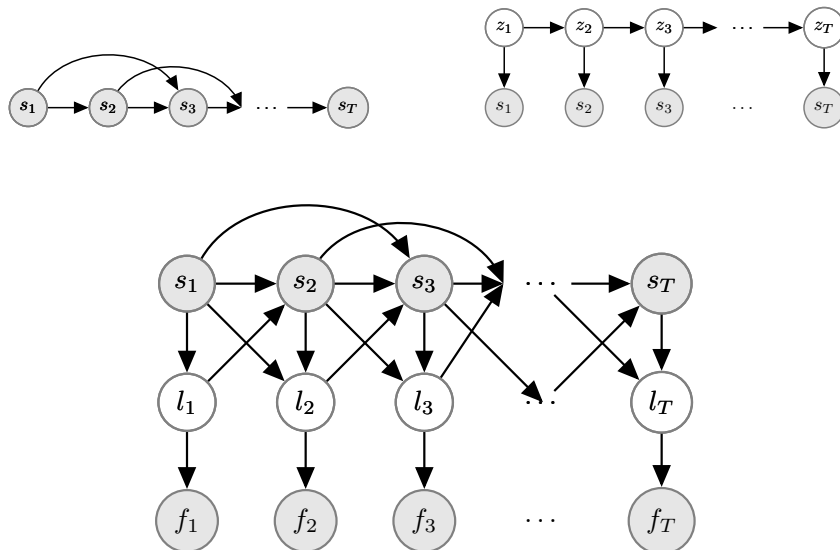


Figure 1: A Markov model (top left) operates solely on the observed states  $s_t$  and easily supports higher-order transition histories, whereas a hidden Markov model (top right) introduces latent states  $z_t$  that govern the transitions but the inference is only efficient for first-order transitions. The partially-hidden Markov model (bottom) introduced in this work combines advantages of both: It supports higher-order transitions but can still take advantage of latent states, though in a different manner than a HMM. In a PHMM the latent states are conditional on the observed state  $s_t$ , and generate an auxiliary representation  $f_t$  instead of the main observed state  $s_t$ .

97 *2.1. Markov Models*

98 Markov models (Figure 1; top left) are tools for modeling fully observed  
 99 sequences of discrete states. Given a sequence  $s_1, \dots, s_T$ , the goal is to learn  
 100 the underlying dynamics in form of the transition probabilities  $p(s_t | s_{t-1})$ . This  
 101 is computationally easy, since the maximum likelihood estimates are obtained  
 102 by merely counting the observed transitions into a  $S \times S$  matrix, where  $S$  is  
 103 the number of different states. Bayesian inference is effectively as easy, using  
 104 Dirichlet priors for the transition probabilities.

105 For many real-word sequences the pure Markovian assumption of the next  
 106 state being conditioned only on the previous one does not hold. Higher-order

107 Markov models relax the assumption by modeling transitions  $p(s_t | s_{t-1}, \dots, s_{t-O})$   
 108 up to some order  $O$ . Even though the transitions probabilities now become ten-  
 109 sors of order  $O + 1$  and hence require more memory, the inference algorithm  
 110 remains the same. For better accuracy with finite data sets the models are  
 111 typically implemented with some sort of backing-off, allowing the model to bor-  
 112 row statistical strength from lower-order history for the rare sequences, which  
 113 increases the complexity of the algorithms but reduces the memory consump-  
 114 tion. The backing-off can be implemented for example by variable order Markov  
 115 models; for nonparametric Bayesian examples, see [15] and [10].

## 116 2.2. Hidden Markov Models

A hidden Markov model (HMM) (Figure 1; top right) generalizes Markov  
 models by coupling the observed states  $s_t$  with latent states  $z_t$ . The Markovian  
 dynamics are assumed for the latent states, so that  $z_t$  depends on  $z_{t-1}$ , and the  
 observed states are emitted by the latent states:

$$z_t | z_{t-1} \sim \pi_{z_t},$$

$$s_t | z_t, \theta \sim F(\theta_{z_t}).$$

117 Here  $\pi_z$  is a vector of probabilities for the  $K$  possible latent states, and  $F(\theta_z)$   
 118 is some density over the space of the observed states, parameterized by  $\theta_z$ .

119 HMMs are more expressive than MMs, but it comes with a notable increase  
 120 in computational cost: The latent state sequence  $z_1, \dots, z_T$  needs to be inferred  
 121 in addition to the transition probabilities, and these two tasks are coupled in a  
 122 manner that typically requires alternating algorithms.<sup>1</sup>

123 Ideally the whole latent state sequence is inferred at once, using dynamic pro-  
 124 gramming [11]. For sampling-based Bayesian inference the algorithm is called  
 125 Forward-Filtering Backward-Sampling (FFBS). Importantly, this part of the in-  
 126 ference algorithm has computational complexity  $\mathcal{O}(TK^2)$ , where  $T$  is the length

---

<sup>1</sup>See [16] for a closed-form solution that requires access to highly accurate estimates of multivariate densities.

127 of the sequence and  $K$  the number of the latent states. In practice HMMs are  
128 only applicable for first-order histories because of this term; for completing the  
129 forward-backward inference for an  $O$ th order model the complexity would be  
130  $\mathcal{O}(TK^{O+1})$ , which quickly becomes infeasible, often already for the 2nd order.

131 Both MMs and HMMs, as well as the PHMM introduced in this work, are  
132 special cases of dynamic Bayesian networks [17]. Even though all of them can  
133 be presented in this general framework, the special cases typically result in con-  
134 siderably more efficient inference and hence dedicated solutions are important.  
135 In our case, the notable advantage compared to generic formulation is that the  
136 conditional independence assumptions made on the latent states enable efficient  
137 nonparametric treatment where the cardinality of the latent states is learned au-  
138 tomatically. To our knowledge, no generic inference solutions for nonparametric  
139 dynamic Bayesian networks have been presented.

### 140 2.3. Hierarchical Dirichlet Process

141 HMMs, as well as PHMMs, assume the data is generated by some unknown  
142 number of latent states  $K$ . While the number  $K$  could be manually set by  
143 the analyst, an interesting alternative is to infer the number directly based on  
144 the data using nonparametric Bayesian modeling techniques. Here we briefly  
145 review the nonparametric model of hierarchical Dirichlet process (HDP) [12],  
146 which has been used to implement nonparametric HMMs [18, 19, 14]. Later we  
147 will use tools belonging to the same family to create a nonparametric version of  
148 the proposed model.

149 Dirichlet process (DP) is a stochastic process that provides densities of the  
150 form  $f(\theta) = \sum_{k=1}^{\infty} \pi_k \delta_{\theta_k}(\theta)$ , where  $\delta$  is the delta measure and  $\pi_k$  sum upto one.  
151 A draw from such a process is denoted by  $G \sim DP(\alpha \mathbf{H})$ , where  $\mathbf{H}$  is a density  
152 from which the  $\theta_k$  are drawn, and  $\alpha$  is a concentration parameter that controls  
153 the decay of the weights  $\pi_k$ . In other words, DP gives a countably infinite  
154 collection of atoms, weighted points in some space, and can hence be used for  
155 example for creating mixture models: Instead of assuming a fixed mixture of  $K$   
156 components, we can use a DP to generate infinitely many of them, of which only

157 a finite set is still needed for modeling any finite data collection. This enables  
158 efficient inference [12].

159 A hierarchical DP (HDP) extends DPs into a hierarchy, generating parallel  
160 DPs that share the same atoms but that can have different weights for them.  
161 In the simplest form the hierarchy is stated as

$$G \sim DP(\alpha\mathbf{H}), \quad G_j \sim DP(\beta G).$$

162 The lower level DPs use  $G$  as their prior, which necessarily implies the  $\theta$  drawn  
163 from them are part of the discrete set provided by  $G$ , and hence the different  
164  $G_j$  share the same atoms, where  $G_j$  is the  $j^{\text{th}}$  random probability measure that  
165 shares atoms with the base measure  $G$ . Since a HMM can be re-formulated  
166 as a collection of mixture models where the mixture weights depend on the  
167 previous mixture allocation, the HDP construction can be used to implement a  
168 nonparametric HMM [18, 19, 14].

### 169 3. Partially Hidden Markov Model

170 In this work we propose a novel family of partially hidden Markov models  
171 for modeling discrete sequences with associated feature vectors, illustrated in  
172 Figure 1 (bottom). The input is given as sequences of observations denoted by  
173  $x_1, x_2, \dots, x_T$ , where each time instance is determined by a tuple  $x_t = (s_t, f_t)$ .  
174 The first element  $s_t$  is a discrete state, whereas the second element  $f_t$  is a  
175  $D$ -dimensional feature vector providing (typically real-valued) auxiliary side in-  
176 formation for that state. In our application the former corresponds to the grid  
177 cell the user is in, and the latter to summary statistics of the movement pattern  
178 within the cell. Both  $s_t$  and  $f_t$  are observed.

179 A regular Markov model would model such data by ignoring  $f_t$  completely,  
180 simply modeling  $s_t$  conditional on some  $O$ th order history of previous locations.  
181 This is naturally sub-optimal, since it completely ignores the features. Another  
182 classical alternative for modeling such sequences would be a HMM, which would  
183 have a set of  $K$  latent states that would emit the whole tuples  $x_t$ . In a straight-  
184 forward application of HMM, each latent state could hence generate several cell



185 locations, and hence the latent states could not be directly interpreted as lo-  
 186 cation information. Furthermore, inference for HMMs is only feasible for very  
 187 low-order transition histories, typically the first order.

188 To combine the advantages of both classical alternatives, we model the se-  
 189 quences with a model we call partially hidden Markov model (PHMM). As  
 190 regular MMs, it supports efficient inference for higher order transitions and di-  
 191 rectly models the observed state sequence  $s_t$ . At the same time, it inherits from  
 192 HMMs the capability of modeling also the associated feature vectors  $f_t$  with  
 193 a collection of latent states  $l_t^{s_t}$ . An important difference to HMMs is that the  
 194 latent states are conditional on the observed state  $s_t$ .

The basic formulation of the model is given by

$$\begin{aligned}
 s_t &\sim p(s_t | l_{t-1}^{s_{t-1}}, s_{t-1}, s_{t-2}, \dots, s_{t-O}), \\
 l_t^{s_t} &\sim p(l_t^{s_t} | l_{t-1}^{s_{t-1}}, s_t, s_{t-1}), \\
 f_t &\sim p(f_t | l_t^{s_t}),
 \end{aligned}
 \tag{1}$$

195 with additional special cases for the first time points, not written out here for  
 196 brevity. In verbal terms, the feature vector itself depends only on the latent  
 197 state, the latent state depends on the previous latent state and the previous cell  
 198 (and naturally also on the current cell, since each cell has its own set of latent  
 199 states), and finally the next cell depends on the previous latent state and the  
 200  $O$ th order history of the cell locations. The use of only first-order history for  
 201 the latent states themselves is crucial for efficient inference of the latent states,  
 202 yet the whole model exhibits higher-order transitions efficiently because of the  
 203 transitions for  $s_t$ .

204 The full model, developed in the next sections, instantiates a nonparametric  
 205 Bayesian version of this basic pattern by coupling the transition probabilities  
 206 with suitable prior distributions, inferring the number of local states for each  
 207 cell nonparametrically, and by hierarchically sharing the latent states of different  
 208 locations.

209 *3.1. Nonparametric PHMM*

210 In the following, we will provide the details on how to implement PHMM  
211 using nonparametric Bayesian tools for automatically inferring the number of  
212 latent states required for each of the observed states  $s_t$ . Since the latent states  
213 are conditional on the observed ones, a parametric model would require setting  $S$   
214 different complexity parameters manually. Unless assuming the same cardinality  
215 for each observed state, this would render tools like cross-validation completely  
216 infeasible. Consequently, nonparametric inference is particularly important for  
217 this model class.

218 A simple mixture density for  $f_t|s_t$  could be implemented with a DP prior.  
219 Sharing the clusters across the observed states would require a HDP instead [12],  
220 as would taking time dependencies into account as in HDP-HMM [18]. Since  
221 our model combines both elements, we will need yet another hierarchical layer,  
222 for which we adopt the tree-HDP construction [13]. In the following we present  
223 the details of these constructions only to the extent it is necessary for deriving  
224 the eventual sampling equations for the proposed model; for formal treatment  
225 of the random processes the reader should consult the original sources.

226 The full model, illustrated in Figure 2, is a single tree-HDP with three layers.  
227 At the highest level stand a collection of global latent states with associated  
228 weights, drawn from the top-level DP. At the next level are  $S$  collections of local  
229 latent states ( $l$ ), one for each geographic cell. These use the global collection  
230 as their prior, which means they share identities but have different weights.  
231 Typically, each local collection uses only a subset of the global states.

232 Finally, the conditional transformations are tied to each other so that all  
233 incoming transitions to a cell  $s$  use the local latent state collection as their prior.  
234 This means that only the latent states present in that cell can be reached, and  
235 that the weights of incoming transitions ( $\pi$ ) are regularized towards each other.  
236 In the end each local state generates a feature vector ( $f$ ). The generating  
237 distribution can be arbitrary, but in our work we use multivariate Gaussian  
238 emissions.

The formal notation for the model can be constructed as a special case of

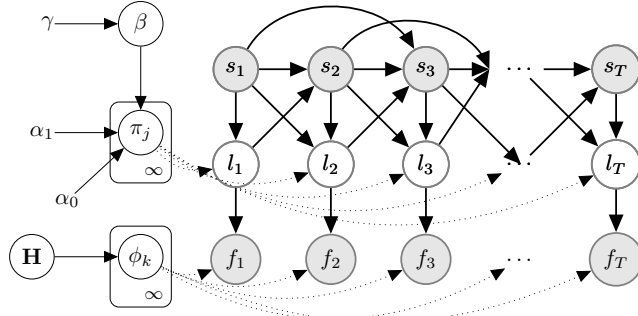


Figure 2: Plate diagram of the nonparametric partially hidden Markov model. The nodes at the left indicate the three levels of the tree-structured HDP construction,  $l_t$  are latent states, and the shaded nodes correspond to the observed coarse locations  $s_t$  and the associated feature vectors  $f_t$ .

the tree-HDP model [13]. Tree-HDP extends HDPs into general tree structures, whereas the model used here is a specific simple tree with three layers, defined as

$$\begin{aligned}
 G_0 &\sim DP(\gamma \mathbf{H}), \\
 G_s &\sim DP(\alpha_0 G_0), \\
 G_{is} &\sim DP(\alpha_1 G_s).
 \end{aligned}$$

239 Here  $H$  is a base measure over the feature vector space,  $G_0$  is the root-level DP  
 240 that provides the global latent states, and  $G_s$  correspond to the collections of  
 241 latent states for each cell. Given a grid of  $S$  cells, there are  $S$  of these collections.  
 242 Finally,  $G_{is}$  refers to one particular incoming transition from a neighboring cell  
 243 to the  $s$ th cell. Here  $i$  is an implicit index that runs over the possible states from  
 244 where one can reach the  $s$ th cell; each  $i$  corresponds to an  $O$ th order sequence  
 245 of cells combined with the latent state of the previous time index.

246 One approach for understanding the fairly abstract formulation above is to  
 247 think in terms of the analogous finite model. Then we would simply have  $K$   
 248 global latent states with emission distributions drawn from the prior  $H$  and  
 249 weights following a Dirichlet distribution. For each cell  $s$  we would then have

250 Dirichlet-distributed weights using the global weights as their prior, and fi-  
 251 nally for all incoming transitions to that location the probabilities would again  
 252 be Dirichlets, this time using the local weights as their prior. In practice  
 253 the nonparametric construction can also be implemented in a similar fash-  
 254 ion, using the stick-breaking construction [20]; the finite Dirichlets are replaced  
 255 with infinite ones parameterized via sticks drawn from beta-distributions. We  
 256 denote the global sticks by  $V_k \sim \text{Beta}(1, \gamma)$  and the associated weights by  
 257  $\beta_k = V_k \prod_i^{k-1} (1 - V_i)$ , the cell-level sticks by  $v_{jk} \sim \text{Beta}(\alpha_0 \beta_k, \alpha_1 (1 - \sum_{l < k} \beta_l))$   
 258 and the corresponding weights by  $p_{jk}$ , and finally the sticks and weights cor-  
 259 responding to the transitions by  $a_{ijk} \sim \text{Beta}(\alpha_1 p_{jk}, \alpha_1 (1 - \sum_{l < k} p_{jl}))$  and  
 260  $\pi_{ijk} = a_{ijk} \prod_{l < k} (1 - a_{ijl})$ . For derivations of these exact forms, see [12, 13].

### 261 3.2. Inference

262 Given a collection of observed sequences, we infer the model parameters by  
 263 Gibbs sampling. The whole inference process is split into two separate parts:  
 264 Inference of the latent state sequences given the rest of the parameters, and  
 265 inference of the parameters given the state sequences.

266 Given the latent state sequences the inference details follow from [13], since  
 267 the model is a special case of their tree-HDP model. Despite the somewhat  
 268 complicated machinery required for correctly handling the nonparametric na-  
 269 ture of the model, the updates for the model parameters still depend only on  
 270 aggregate count statistics as they would for a parametric model.

271 We denote by  $N_j$  the total number of incoming transitions into the  $j$ th grid  
 272 cell, and by  $n_{ijk}$  the number of those coming from the  $i$ th history and using  
 273 the global latent state  $k$ . Furthermore, we denote by  $m_{jk}$  the total number  
 274 of latent states at the grid cell level  $G_j$  that are assigned to the global latent  
 275 state  $k$ . The quantities  $n_{ijk}$  and  $m_{jk}$  are not fully observed, but instead need  
 276 to be sampled as explained by [13]. Finally, the transition counts  $t_{gjdkl}$  are the  
 277 number of transitions from the  $g$ th grid cell using the latent state  $l$  to the  $j$ th  
 278 grid cell using the latent state  $k$ . Given the above aggregate statistics, the model  
 279 parameters can be sampled as follows:

- 280 1. Break more sticks at the global level to support creation of new states at  
 281 lower levels:

$$\beta | \gamma \sim \text{Stick}(\gamma)$$

2. Update the global weights:

$$P(m_{jk} = m) \propto s(m_{jk}, k) \cdot (\alpha_0 \beta_k^{old})^m$$

$$v_k = \sum_j m_{jk}$$

$$\beta_k \sim \text{Dirichlet}(v_1, \dots, v_k, \gamma)$$

3. Update the cell weights:

$$P(n_{ijk} = n) \propto s(n_{ijk}, k) \cdot (\alpha_1 \beta_{jk}^{old})^n$$

$$l_{jk} = \sum_i n_{ijk}$$

$$\beta_{jk} \sim \text{Dirichlet}(l_{j1}, \dots, l_{jk}, \alpha_0 \beta_k^{old})$$

4. Update the transition probabilities:

$$\pi_{gjl} \sim \text{Dirichlet}(t_{gjl1}, \dots, t_{gjlk}, \alpha_1 \beta_{jk}^{old})$$

282 Here  $s(n, k)$  denotes the Stirling numbers of the first kind; see [13] for further  
 283 explanation.

284 Given the current values for the transition probabilities we then sample the  
 285 full state sequence of  $T$  elements at once. Even though the model is not a  
 286 HMM, we can perform this stage using an analogous forward-backward sam-  
 287 pling procedure since the transitions depend only on the previous latent state  
 288 and not longer history of those. As we recall from Section 2, the complexity  
 289 of this depends on the number of latent states, which here is unbounded. The  
 290 first HDP-HMM models circumvented this by not sampling the whole sequence  
 291 at one go, but the beam sampler by [14] showed how we can not only perform  
 292 forward-backward sampling for HDP-HMM but in fact can often do it with less  
 293 computational demand compared to a regular HMM with similar state cardi-  
 294 nality; only transitions with sufficiently high probability need to be considered,

295 which often means considerably less computation in total.

296 We extend the beam sampler of [14] for our model as follows. We denote  
 297 by  $s_t$  the grid cell at time  $t$ , and by  $l_t$  the corresponding latent state, and for  
 298 brevity denote  $(s_t, l_t)$  by  $h_t$ .

Following the basic idea of beam sampling (and slice samplers in general), we draw an auxiliary slice variable  $u_t \sim \text{Uniform}(0, \pi_{h_{t-1}, h_t})$  for each time point to represent the lowest transition probability that need to be considered, adaptively truncating the model to a finite one for the purpose of this step alone. The forward filtering step can then be written as

$$\begin{aligned} P(h_t | x_{1:t}, u_{1:t}) &\propto P(h_t, u_t, x_t | x_{1:t-1}, u_{1:t-1}) \\ &= P(x_t | h_t) \sum_{h_{t-1}} \mathbb{1}(u_t < \pi_{h_{t-1}, h_t}) P(h_{t-1} | x_{1:t-1}, u_{1:t-1}) \\ &= P(x_t | h_t) \sum_{h_{t-1}: u_t < \pi_{h_{t-1}, h_t}} P(h_{t-1} | x_{1:t-1}, u_{1:t-1}), \end{aligned}$$

and the backwards sampling is performed by

$$h_t \sim P(h_t | x_{1:t}, u_{1:t}) P(h_{t+1} | h_t, u_{t+1}).$$

299 Note that this adaptive truncation is not a heuristic strategy, but the slice sam-  
 300 pling technique indeed draws samples from the correct posterior. Furthermore,  
 301 we typically need to consider only a small subset of the states for each summa-  
 302 tion above; see [14] for details.

#### 303 4. Illustration

304 To illustrate the basic behavior of the model, we apply it on four different  
 305 artificial data sets generated from a parametric version of the PHMM model,  
 306 assuming a set of  $S = 6$  discrete states (cells). The four data sets showcase in-  
 307 creasingly more complex dynamics, the easiest corresponding to regular Marko-  
 308 vian assumption and the last one corresponding to second-order Markovian  
 309 transitions further conditioned on  $K = 5$  latent states associated with each cell.  
 310 The generative process is exactly as described in (1), where we draw the tran-  
 311 sition probabilities for both  $s$  and  $l$  from Dirichlet distributions with the prior

Table 1: Predictive accuracy (in percentages) of the proposed partially observed Markov model (PHMM) and the baseline of regular Markov model (MM) on four artificial data sets. For the data sets with only one latent state ( $K=1$ ) the models are equivalent, as they should, but for cases with more latent states ( $K=5$ ) PHMM outperforms MM that ignores the auxiliary features. The table also shows the models restricted to only first order histories are not as accurate if the data exhibits second order transitions ( $O=2$ ), motivating the support for higher-order dynamics. The boldface font indicates for each data set the best methods for which the performance is indistinguishable; the small deviations are because of random fluctuation.

Artificial Data	MM-1	MM-2	PHMM-1	PHMM-2
$O = 1, K = 1$	<b>92.3</b>	<b>92.2</b>	<b>91.9</b>	<b>92.5</b>
$O = 1, K = 5$	34.5	44.0	<b>65.7</b>	<b>64.5</b>
$O = 2, K = 1$	33.8	<b>63.7</b>	34.1	<b>62.3</b>
$O = 2, K = 5$	28.4	40.3	46.3	<b>65.4</b>

parameter 0.1, in order to create distributions that deviate notably from uniform density. For the cases with latent states the emissions  $p(f_t|l_t)$  are normal distributions with means  $(-5, -2.5, 0, 2.5, 5)$  and shared standard deviation 1.

We applied four alternative models on each of the data sets: MM-1, MM-2, PHMM-1, and PHMM-2, where the number after the dash denotes the order of the model. These correspond exactly to the requirements of the four data sets; all four methods should solve the first data sets, whereas only the last one is flexible enough to model the most complex data set. We train the models using a sequence of 5,000 samples drawn from the model and evaluate them using the predictive accuracy on a separate test sequence of 5,000 samples, for the task of identifying the next cell. Table 1 shows the methods work as expected; PHMM-2 is superior for the data that requires 2nd order dynamics and latent states. The simpler data sets can be modeled correctly by some of the alternatives as well, but notably PHMM-2 is always on par with the best ones. We also confirmed that the nonparametric PHMM models correctly learnt the number of the latent states, and that the best methods reach the optimal accuracy obtained when predicting with the true generating model.

329 Finally, we also tried higher-order MMs for the last data set to study whether  
330 the lack of latent states can be compensated by considering even longer histories  
331 on the observed states. The accuracy of MM indeed goes up for higher orders,  
332 reaching 50.8% for MM-3 and 48.0% for MM-4, but PHMM-2 still outperforms  
333 these clearly while requiring smaller transition tensors than MM-4. The same  
334 effect is visible already in the  $O = 1, K = 5$  case where MM-2 outperforms  
335 MM-1.

336 To summarize the results, PHMM reached the best accuracy in all experi-  
337 ments; for the more complex data sets it outperformed the simpler alternatives,  
338 but even for the simpler generative processes it reached the same accuracy and  
339 hence the only drawback is in additional computational cost. Importantly, MMs  
340 with even higher order transitions were not as accurate as PHMMs.

## 341 5. Modeling Indoor Movement

342 The main application motivation for this work is in modeling indoor move-  
343 ment while preserving the privacy of the clients. Typical end-use scenarios for  
344 such models are in understanding how people behave in public spaces such as  
345 shopping centers, museums, or office buildings. For all these cases the owners  
346 of the premise are interested in understanding the flows and making predictions  
347 to support location-based services and to dynamically allocate resources, for ex-  
348 ample by opening more counters based on the predicted movement patterns. At  
349 the same time, these are all examples where the owner has no need to know the  
350 exact locations of the individuals, and it is reasonable to actively prevent them  
351 from being able to spy on them by never storing the detailed location data.

### 352 5.1. Data and feature representation

353 We apply the model in a retail environment, modeling location data col-  
354 lected in a hypermarket by tracking shopping carts and baskets with a com-  
355 mercial high-accuracy positioning system (HAIP) provided by Quuppa. The  
356 system tracks small Bluetooth Smart chips integrated in the carts and baskets,



357 providing accurate (error less than 1 meter) position with 10Hz frequency. We  
358 model the data at granularity of 20x20 meter coarse locations, to get a rough  
359 overview at a departmental level, using a total of 1,839 sequences collected dur-  
360 ing a period of 30 days.

361 At the core of the PHMM model are the aggregate summaries collected  
362 based on the more detailed location data, stored to accompany each time point  
363 of the coarse trajectory. In this work we present a few simple alternative rep-  
364 resentations, primarily to demonstrate that the more accurately the aggregate  
365 characteristics capture the nature of the movement within the coarse location,  
366 the better the overall model will be.

367 These representations are not specifically tuned for our evaluation, since the  
368 idea is that the features would be extracted already before handing the data  
369 for someone that learns the actual model and hence they should be generally  
370 applicable for various kinds of modeling tasks.

371 We compute a set of eight basic features (Table 2). These features ex-  
372 tract natural elements about the movement, covering aspects like the amount  
373 of time spent ( $\Delta t$ ), how often the person stopped (for example to pick items  
374 from the shelves; Pauses), and characterizations of their general movement di-  
375 rection ( $\Delta X_+$ ,  $\Delta X_-$ ,  $\Delta Y_+$ ,  $\Delta Y_-$ ). All of these features are privacy-preserving  
376 in the sense that they do not reveal the precise location of the person at any  
377 point. For illustrating the effect of the quality of the local representation, we  
378 then construct alternative feature sets as subsets of these eight basic features.  
379 The simplest set includes just the time spent (corresponding to a semi-Markov  
380 model), whereas the best coverage is obtained by using all of them. Besides  
381 these extremes, we also ran experiments with two intermediate collections.

## 382 5.2. Experiments

383 The PHMM model has two core elements that control its expressive power:  
384 The maximum order of transition history with respect to  $s$ , and the accuracy of  
385 the feature vector  $f$  in characterizing the local movement behavior. To illustrate  
386 how the model behaves with respect to these two elements, we first conduct

Table 2: Description of the features used for characterizing the local movement patterns. Each feature describes the movement within the cell, and hence for example the mean coordinates are with respect to the origin of the grid cell.  $\Delta X_+$  and  $\Delta X_-$  correspond to the distances moved in positive  $X$  direction and negative  $X$  direction respectively. Similarly, we have  $\Delta Y_+$  and  $\Delta Y_-$ .

$\Delta t$	Logarithm of the total time spent
$\Delta X_+, \Delta X_-, \Delta Y_+, \Delta Y_-$	Total distance moved rightwards, leftwards, upwards, downwards
$M_x, M_y$	Mean of the x and y
Pauses	Total number of stops or pauses

387 separate experiments for each of them in isolation. After demonstrating that  
 388 improving either element indeed results in better predictive accuracy, we present  
 389 the results for a model that uses the best choices for both elements.

390 For all models we measure the accuracy using a setup where 1,471 trajec-  
 391 tories are used for training and 368 trajectories are used for testing. We train  
 392 the model using the training trajectories, running the Gibbs sampler for 2,000  
 393 iterations and discarding the first 1,500 samples as burn-in. For each test tra-  
 394 jectory we randomly sample a time of prediction, meaning that we assume we  
 395 have recorded the trajectory up to that point and then need to predict the next  
 396 few locations. For the observed part we infer the latent trajectory as we do for  
 397 the training samples, and we then predict the future points using simple forward  
 398 sampling: We instantiate 100 particles for each test sequence, propagate them  
 399 forward in time using the transition probabilities, and finally compute the ac-  
 400 curacy by averaging over the predictions of these particles. The accuracy score  
 401 is defined as the ratio of these particles that fall to the exact correct grid cell.

402 Figure 3 illustrates the complete modeling pipeline, showing both how indi-  
 403 vidual trajectories are represented using grid cells and feature vectors, as well  
 404 depicting the training and test procedure described above.

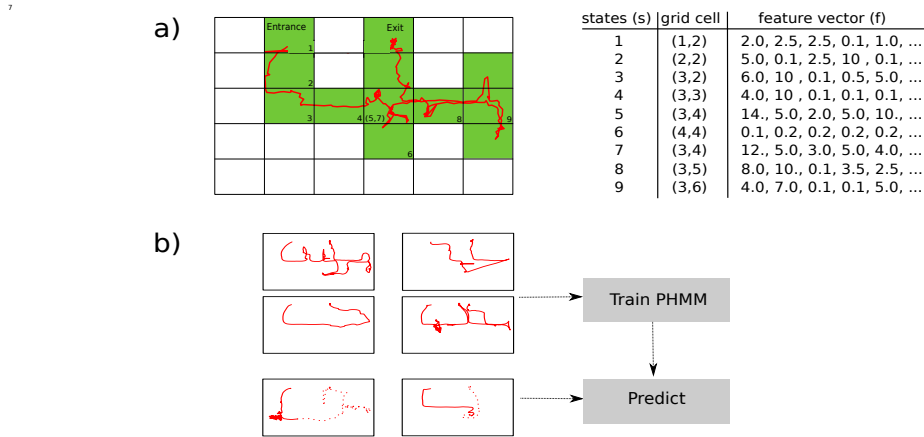


Figure 3: Illustration of the way the PHMM model is applied for modeling indoor trajectories in a privacy-preserving manner. **a)** Every path is pre-processed by extracting the grid cell identifiers for all distinct visits to individual cells, and for each visit we compute the feature vector representation characterizing the nature of the movement within the cell. **b)** We use 75% of the path sequences for training, utilizing the full trajectories. The empirical performance of the model is then evaluated in a prediction task: For the remaining 25% of sequences we observe the sequence only upto a randomly determined time point, and attempt to predict the remaining steps along the sequence, indicated here by the dotted lines.

405 *5.2.1. Higher-order History*

406 We start the experiments by looking at a special case of PHMM with no  
 407 local states, which corresponds to a regular MM. This experiment is conducted  
 408 to verify that higher-order transitions indeed are useful for this kind of data.  
 409 Figure 4 (left) shows that 2nd order MMs are considerably more accurate than  
 410 1st order, but there is no notable difference between 2nd order models and the  
 411 ones with even higher order on this data. Based on this observation, we will use  
 412 2nd order history for the final PHMM model, as the lowest complexity choice  
 413 of the well-performing ones.

414 *5.2.2. Local Pattern Models*

415 The more interesting element of the PHMM model is the local feature de-  
 416 scription and the associated local states. Here we experiment with increasingly  
 417 more complex feature descriptions, keeping the order of the model fixed to one,

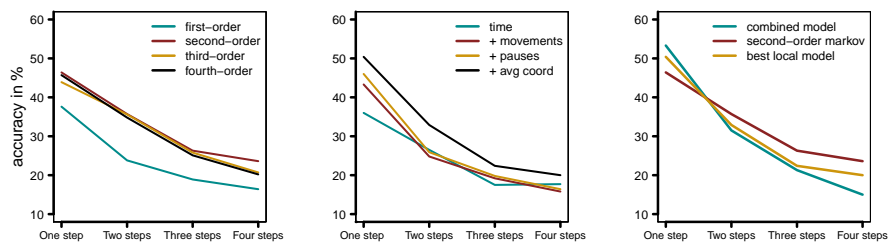


Figure 4: **Left:** 2nd order Markov models are clearly more accurate than 1st order models, but on this data the higher order ones do not help. **Middle:** More descriptive local feature representations improve the accuracy of a 1st order PHMM. Merely knowing the time the user spent in the grid location does not help much compared to no local states (see the left sub-figure), but all additional features improve the accuracy. **Right:** Combining the 2nd order history with the best local model further improves the accuracy for short-term predictions, but not for long-term ones. In all three sub-plots the x-axis denotes how many time-points in future we are predicting and the y-axis indicates the accuracy of making exactly the right prediction.

418 to show that knowing more about the fine movements within the grid cell helps  
 419 creating more expressive models.

420 The more interesting element of the PHMM model is the local feature de-  
 421 scription and the associated local states. Here we experiment with increasingly  
 422 more complex feature descriptions, keeping the order of the model fixed to one,  
 423 to show that knowing more about the fine movements within the grid cell helps  
 424 creating more expressive models.

425 Figure 4 (middle) shows prediction accuracies for four model variants. The  
 426 first variant has very simple feature representation (only the time spent in the  
 427 cell), whereas all others progressively add more features. The best accuracy is  
 428 obtained with the model that has the most features, which confirms the intuitive  
 429 expectation.

430 To further understand the difference between the different local models, we  
 431 can inspect the number of global latent states the nonparametric formulation  
 432 learns for each of them. These also go up when the feature description contains  
 433 more information, from 6 to 24 (averaged over the posterior samples; note that  
 434 none of the cells actually use all of these) when going from the simplest repre-

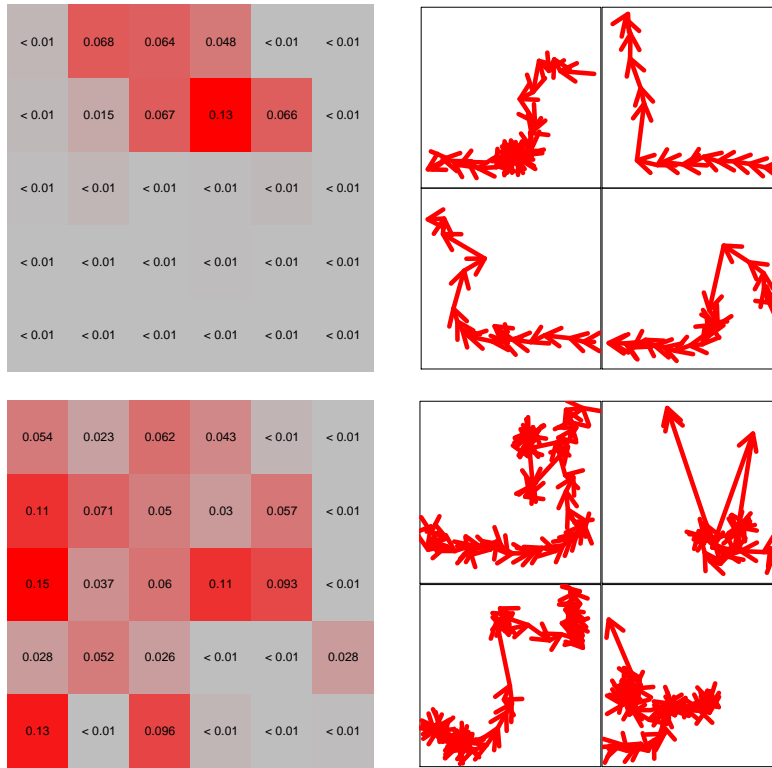


Figure 5: Illustration of prevalences of movement patterns across the hypermarket. The pattern on the top row corresponds to primarily leftwards movement carried out without notable pauses, illustrated for examples on the right. The heatmap on the left shows the pattern is primarily used in the top-most areas of the store, near the counters, and it corresponds to customers walking in front of the counters towards one with a short queue. The other example shown on the bottom row corresponds to more complex movement pattern within a grid cell, revealing multiple stops or reversals. This pattern is frequent in the left side of the store, which contains clothes and other items the customers often browse for a longer time. The heatmaps show the cell-level probabilities acting as the prior for all incoming transitions, roughly corresponding to the ratio of partial trajectories belonging to this particular latent state; both of these patterns explain 10-15% of the local movement patterns in the most common cells.

435 sentation to the most complex. Intuitively, there is no need for multiple local  
 436 states when the feature descriptions are not expressive, whereas more states can  
 437 be used to differentiate between different movement patterns when the feature

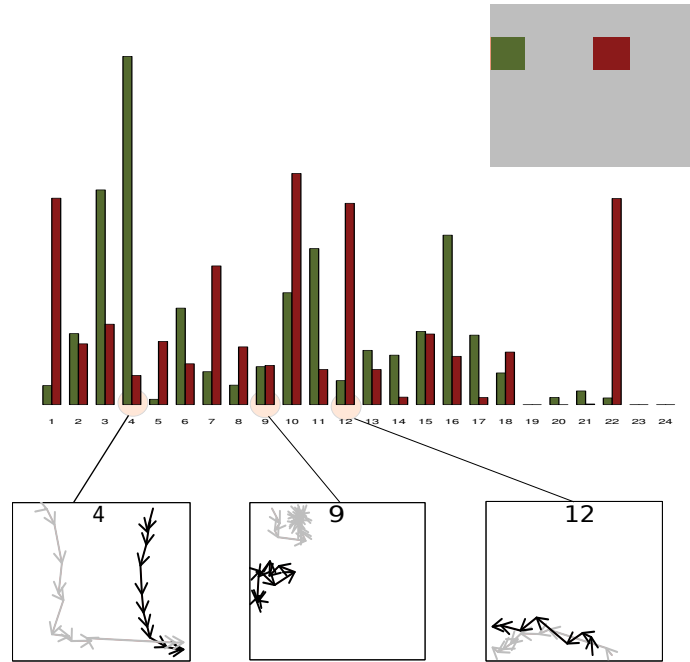


Figure 6: Illustration of PHMM in analysis of indoor movement. The grid on the top-right corner shows the discretized store layout, and we have chosen two cells (green and red) for illustrating the model. This posterior sample contains 24 global latent states shared by all cells (ordered in decreasing global probability  $\beta_k$ ), and the bar plot in the middle shows the local probabilities  $p_{jk}$  of these two cells. We see that infrequently used global states (states from 19 to 24) have on average lower weights for these cells and some rare states can also have high probability in specific cells (like state 22 for the red cell). To further illustrate the results we show three latent states in more detail, presenting two example path snippets falling into each of these. State 4 has high probability in the green cell and corresponds to downwards movement that eventually turns left; it is almost absent in the red cell that has no corridors like this. State 9 corresponds to a pattern where the customer stops to inspect something, and it is present in both cells. Finally, state 12 corresponds to leftwards movement and naturally has low probability in the green cell since the store ends on its left side. Even though we here illustrated the actual path snippets for visualization purposes, it is good to remember the model itself only knew about the summary statistics.

438 vector is rich.

439 *5.2.3. Combination*

440 Given the above results indicating that higher-order history and accurate  
441 local feature representations are beneficial, we run the final experiments with a  
442 PHMM model that uses 2nd order history and the most complex representation  
443 for the local movements.

444 Figure 4 (right) collects the predictive accuracies of the earlier special cases  
445 together with this final model, showing that for predicting the immediate next  
446 grid cell the combination provides the best accuracy. For longer-term predictions  
447 it is only on par with the PHMM using 1st order history, and in fact less accurate  
448 than a standard 2nd order MM. However, it is important to note that predictive  
449 accuracy is here merely a proxy for roughly evaluating the models, and not the  
450 end goal of our work as such. Even though the PHMM model is only comparable  
451 to the alternatives in pure predictive accuracy, its primary use is in describing  
452 the movement patterns, which we will illustrate next.

453 The only way to interpret a Markov model is to inspect the transition prob-  
454 abilities, which becomes cumbersome especially when looking at higher order  
455 transitions, whereas HMMs would not directly associate the latent states with  
456 the grids. PHMM, in turn, provides latent states for each grid cell and the states  
457 share identities across different cells. Each latent state is also coupled with a  
458 prototypical feature vector that describes a movement pattern within the cell.  
459 By inspecting the probabilities of the different local states across the space we  
460 can easily identify areas where people exhibit certain type of behavior. We  
461 present an brief example of such analysis in Figure 6, showing example latent  
462 states for two distinct locations of the store. We also show a spatial distribution  
463 of the usage of a particular latent state, and examples of real trajectory pieces  
464 mapped to these latent states in Figure 5 More detailed analysis of the move-  
465 ment patterns within the undisclosed market studied here is outside the scope  
466 of this publication.

## 467 6. Conclusion

468 In this work we studied Markovian models for privacy-preserving modeling of  
469 indoor movement patterns in a fixed physical space. Instead of directly modeling  
470 high-accuracy positioning traces, we model the movement patterns at a level of  
471 a coarse grid, representing the fine movements with the grid cells via aggregate  
472 feature vectors. This way the detailed locations of the user are not revealed for  
473 the analyst, yet some information about them enters the model.

474 To model sequences of observed grid locations and the associated feature  
475 vectors, we proposed novel partially-hidden Markov model, which borrows ele-  
476 ments both from higher-order Markov models and hidden Markov models. It  
477 supports transitions that take into account higher-order dynamics in terms of  
478 the observed grid locations, but still can infer the latent states associated with  
479 them with a forward-backward step that is as efficient to compute as the cor-  
480 responding algorithm for HMMs. We instantiated a nonparametric Bayesian  
481 version of the general model structure, using tools from tree-structured HDPs  
482 [13] and beam sampling [14] for inference.

483 We demonstrated on real trajectory data collected in a hypermarket that  
484 the proposed model is suitable for this kind of data, and that both good-quality  
485 auxiliary features and higher-order transitions are needed for interpretable sum-  
486 maries that are also predictive of future movement. While a regular higher-order  
487 Markov model provides predictions of comparable accuracy, it does not provide  
488 the latent states that describe typical movement patterns in different parts of  
489 the space.

490 The main limitation of the work considers specification of the cell grid un-  
491 derlying the model. Here we used a simple evenly spaced grid that did not take  
492 the layout of the store into account. This sometimes results in spurious back  
493 and forth movement between two cells when cell borders are located on areas  
494 where the users spends time without moving much. Furthermore, the While the  
495 model handles these cases correctly, learning states that correspond to short  
496 visits followed by returning to the previous cell, it has detrimental effect on the



497 prediction accuracy. One potential remedy would be to discard very short visits  
498 as a pre-processing step. Taking the store layout into account when placing the  
499 grid, so that cell borders would typically be along walls or shelves, would help  
500 as well. Finally, an interesting possibility for future work would be to extend  
501 the model to support more flexible cells that would not necessarily fall into a  
502 regular grid but would be designed based on the actual layout.

503 The main focus in this work was in presenting the PHMM model itself and  
504 providing the necessary inference details. For practical applications the feature  
505 representation used for characterising detailed movement within grid cells would  
506 warrant more extensive study; replacing the crude representation used here with  
507 more elaborate descriptions would likely result in improved accuracy with no  
508 additional computation.

#### 509 *Acknowledgments*

510 We acknowledge support from TEKES (Digile SHOK programme D2I) and  
511 Academy of Finland (Finnish Centre of Excellence in Computational Inference  
512 Research COIN, grant 251170; grant 266969).

#### 513 **References**

- 514 [1] H. Liu, H. Darabi, P. Banerjee, J. Liu, Survey of wireless indoor posi-  
515 tioning techniques and systems, *Systems, Man, and Cybernetics, Part C:*  
516 *Applications and Reviews*, IEEE Transactions on 37 (6) (2007) 1067–1080.
- 517 [2] T. Roos, P. Myllymäki, H. Tirri, P. Misikangas, J. Sievänen, A proba-  
518 bilistic approach to wlan user location estimation, *International Journal of*  
519 *Wireless Information Networks* 9 (3) (2002) 155–164.
- 520 [3] O. Woodman, R. Harle, Pedestrian localisation for indoor environments, in:  
521 *Proceedings of the 10th international conference on Ubiquitous computing*,  
522 ACM, 2008, pp. 114–123.

- 523 [4] E. Dahlgren, H. Mahmood, Evaluation of indoor positioning based on Blue-  
524 tooth Smart technology, Master's thesis, Chalmers University of Technol-  
525 ogy (2014).
- 526 [5] J. J. Nielsen, N. Amiot, T. K. Madsen, Directional hidden markov model  
527 for indoor tracking of mobile users and realistic case study, in: European  
528 Wireless 2013; 19th European Wireless Conference, 2013, pp. 1–6.
- 529 [6] J. Yoo, H. J. Kim, K. H. Johansson, Mapless indoor localization by trajec-  
530 tory learning from a crowd, in: 2016 International Conference on Indoor  
531 Positioning and Indoor Navigation (IPIN), 2016, pp. 1–7.
- 532 [7] N. Zeng, H. Zhang, Y. Chen, B. Chen, Y. Liu, Path planning for intelli-  
533 gent robot based on switching local evolutionary pso algorithm, *Assembly  
534 Automation* 36 (2) (2016) 120–126.
- 535 [8] A. Asahara, A. Sato, K. Maruyama, K. Seto, Predestrian-movement pre-  
536 diction based on mixed Markov-chain model, in: *Proceedings of ACM  
537 SIGSPATIAL GIS*, 2011, pp. 25–33.
- 538 [9] R. Begleiter, R. El-Yaniv, G. Yona, On prediction using variable order  
539 Markov models, *Journal of Artificial Intelligence Research* 22 (2004) 385–  
540 421.
- 541 [10] F. Wood, C. Archambeau, J. Gasthaus, L. James, Y. W. Teh, A stochas-  
542 tic memoizer for sequence data, in: *Proceedings of the 26th International  
543 Conference on Machine Learning*, 2009.
- 544 [11] L. R. Rabiner, A tutorial on hidden Markov models and selected applica-  
545 tions in speech recognition, in: *Proceedings of the IEEE*, 1989, pp. 257–286.
- 546 [12] Y. W. Teh, M. I. Jordan, M. J. Beal, D. M. Blei, Hierarchical Dirichlet  
547 processes, *Journal of the American Statistical Association* 101 (476) (2006)  
548 1566–1581.

- 549 [13] K. R. Canini, T. L. Griffiths, A nonparametric Bayesian model of multi-  
550 level category learning, in: Proceedings of the 25th AAAI Conference on  
551 Artificial Intelligence (AAAI), 2011.
- 552 [14] J. Van Gael, Y. Saatchi, Y. W. Teh, Z. Ghahramani, Beam sampling for the  
553 infinite hidden Markov model, in: Proceedings of the 25th International  
554 Conference on Machine Learning (ICML), 2008.
- 555 [15] D. Mochihashi, E. Sumita, The infinite Markov model, in: Advances in  
556 neural information processing systems, 2007, pp. 1017–1024.
- 557 [16] D. Hsu, S. M. Kakade, T. Zhang, A spectral algorithm for learning hidden  
558 markov models, *Journal of Computer and System Sciences* 78 (5) (2012)  
559 1460–1480.
- 560 [17] K. P. Murphy, *Dynamic Bayesian networks: Representation, inference and*  
561 *learning*, Ph.D. thesis, University of California, Berkeley (2002).
- 562 [18] M. J. Beal, Z. Ghahramani, C. E. Rasmussen, The infinite hidden Markov  
563 model, in: *Advances in Neural Information Processing Systems*, 2001, pp.  
564 577–584.
- 565 [19] E. B. Fox, E. B. Sudderth, M. I. Jordan, A. S. Willsky, An HDP-HMM for  
566 systems with state persistence, in: Proceedings of the 25th International  
567 Conference on Machine Learning, ICML '08, 2008, pp. 312–319.
- 568 [20] H. Ishwaran, L. F. James, Gibbs sampling methods for stick-breaking pri-  
569 ors, *Journal of the Americal Statistical Association* 96 (453) (2001) 161–  
570 173.